Ab Initio and Direct Dynamics Studies of the Reaction of Singlet Methylene with Acetylene and the Lifetime of the Cyclopropene Complex

Hua-Gen Yu* and James T. Muckerman‡

Department of Chemistry, Brookhaven National Laboratory, Upton, New York 11973-5000

Received: October 29, 2004; In Final Form: January 4, 2005

The energetics of the $^1CH_2 + C_2H_2 \rightarrow H + C_3H_3$ reaction are accurately calculated using an extrapolated coupled-cluster/complete basis set (CBS) method based on the cc-pVDZ, cc-pVTZ, and cc-pVQZ basis sets. The reaction enthalpy (0 K) is predicted to be −20.33 kcal/mol. This reaction has no classical barrier in either the entrance or exit channel. However, there are several stable intermediates—cyclopropene (c-C_3H_4), allene (CH_2CCH_2), and propyne (CH_3CCH)—along the minimum energy path. These intermediates with zero-point energy corrections lie below the reactants by 87.11 (c-C_3H_4), 109.69 (CH_2CCH_2), and 110.78 kcal/mol (CH_3CCH). The vibrationally adiabatic ground-state (VAG) barrier height for c-C_3H_4 isomerization to allene is obtained as 45.2 kcal/mol, and to propyne as 37.2 kcal/mol. In addition, the $^1CH_2 + C_2H_2$ reaction is investigated utilizing the dual-level "scaling all correlation" (SAC) ab initio method of Truhlar et al., i.e., the UCCSD(SAC)/cc-pVDZ theory. Results show that the reaction occurs via long-lived complexes. The lifetime of the cyclopropene intermediate is obtained as 3.2 ± 0.4 ps. It is found that the intermediate propyne can be formed directly from reactants through the insertion of $^1CH_2$ into a C−H bond of C_2H_2. However, compared to the major mechanism in which the propyne is produced through a ring-opening of the cyclopropene complex, this reaction pathway is much less favorable. Finally, the theoretical thermal rate constant exhibits a negative temperature dependence, which is in excellent agreement with the previous results. The temperature dependence is consistent with the earlier RRKM results but weaker than the experimental observations at high temperatures.

I. Introduction

The $^1CH_2 + C_2H_2 \rightarrow H + C_3H_3$ reaction[1−4] is an important reaction in combustion chemistry as it is the major source of propargyl (C_3H_3) radicals in combustion environments. These radicals are thought to be crucial precursors in the formation of soot. Soot formation starts with a recombination of propargyl radicals to benzene and its isomers,[2,5−8] which further leads to other polycyclic aromatic hydrocarbons (PAH) via addition reactions with other carbon-containing species. It is believed that the formation of the first cyclic C_6 ring is the rate-limiting step in PAH formation.[6]

During the past decade there have been several studies[9−22] on the $^1CH_2 + C_2H_2 \rightarrow H + C_3H_3$ reaction. The stationary points along the minimum energy path have been characterized using different ab initio methods including single-reference self-consistent field (SCF) and multireference configuration interaction (MRCI) methods,[9−11] internally contracted configuration interaction (ICCI) theory,[12,13] and density function theory (DFT) calculations.[14] Results show that the reaction prefers to occur via the long-lived intermediates cyclopropene (c-C_3H_4), allene (CH_2CCH_2), and propyne (CH_3CCH). The cyclopropene molecule is first formed by the addition of singlet methylene to the carbon−carbon triple bond in acetylene. It is a barrierless process. Then a ring-opening reaction of c-C_3H_4 can lead to isomerization either to the allene or propyne molecule. Both molecules are very stable intermediates, which eventually dissociate into the $H + C_3H_3$ products in a collision-free environment.

The overall rate constant for the disappearance of $^1CH_2$ in C_2H_2, including the collisionally induced intersystem crossing (CIISC) of $^1CH_2$ to form $^3CH_2$, has been determined as 2.5−3.7 × 10^{-10} cm^3 molecule^{-1} s^{-1} by several groups[16−20] at room temperature. Although the branching fraction into the propargyl radical was not resolved, the branching fraction of CIISC was measured by Hack et al.[19] to be (22 ± 7)%. Unfortunately, those experimental rate constants show apparent pressure dependence. The values obtained are inversely proportional to the experimental pressure.[16−20] This is partially caused by the long-lived intermediates involved in the reaction. According to statistical RRKM simulations,[13−16] these intermediates can be stabilized by a collision process. Importantly, a direct measurement for the $^1CH_2 + C_2H_2 \rightarrow H + C_3H_3$ reaction was made by Adamson et al.[21] using an infrared kinetic spectroscopy technique. They determined a larger rate constant of (3.5 ± 0.7) × 10^{-10} cm^3 molecule^{-1} s^{-1} at 295 K. Recently, the reaction was studied by Davis and co-workers[22] using a crossed molecular beam method at a mean collision energy of 3.0 kcal/mol.

There is only one experimental study[16] of the effect of temperature on the reaction rate constant. Blitz and co-workers observed a negative temperature dependence, which is consistent with the statistical RRKM calculations of Guadagnini, Schatz, and Walch.[13] The latter workers obtained reaction rate constant values of 3.6 × 10^{-10} cm^3 molecule^{-1} s^{-1} at 300 K, and 3.0 × 10^{-10} cm^3 molecule^{-1} s^{-1} at 1000 K, but the theoretical result at the high temperature seems much larger than the experimental value of 1.21 × 10^{-10} cm^3 molecule^{-1} s^{-1} at 773 K. In other words, the experimental results show a stronger negative temperature dependence than predicted by the RRKM studies. Currently, this is still an open question. The RRKM simulations have involved some approximations while the kinetics experiment does not distinguish well the CIISC relaxation of $^1CH_2$ from the chemical reaction.

* Address correspondence to this author. E-mail: hgy@bnl.gov. Fax: +1-631-344 5815.

‡ E-mail: muckerma@bnl.gov.

10.1021/jp045049w CCC: $30.25
Published on Web 02/12/2005

In this work we attempt to resolve this issue unambiguously using an ab initio molecular dynamics method. First, accurate energetics of the critical stationary points on the singlet potential energy surface for the $^1CH_2 + C_2H_2 \rightarrow H + C_3H_3$ reaction are calculated using an extrapolated coupled-cluster/complete basis set (CBS) method. The results are then employed as criteria for selecting a reliable ab initio method to be used in the dynamics calculations. Finally, a direct ab initio molecular dynamics study of the $^1CH_2 + C_2H_2$ reaction is carried out. The temperature dependence of the reaction rate constant from the results of the dynamics study is compared to experiment, and the behavior of the trajectories allows us to analyze the lifetime of the cyclopropene complex and to elucidate the reaction mechanisms.

II. Computational Method

Geometrical optimizations and harmonic normal-mode frequencies at the stationary points on the lowest singlet potential energy surface for the $^1CH_2 + C_2H_2 \rightarrow H + C_3H_3$ reaction are carried out using coupled-cluster theory including single and double excitation terms[23−25] with the correlation consistent double-ζ basis set of Dunning,[26] i.e, the UCCSD/cc-pVDZ method. The energies at the optimized geometries are further corrected for basis set and CI truncation errors. The CI truncation errors are estimated at the UCCSD(T)/cc-pVQZ level.[27,28] The basis set errors are removed using the extrapolation approach of Helgaker and co-workers.[29−31] Here, the cc-pVDZ, cc-pVTZ, and cc-pVQZ basis sets are employed in the extrapolation procedure at the UCCSD(T) theory level. The final complete basis set (CBS) energies can be written as

$$E_{\mathrm{CBSI}}^{\mathrm{W1}} = E_{\mathrm{UCCSD(T)/cc-pVQZ}} + 0.6556343(E_{\mathrm{UCCSD(T)/cc-pVQZ}} - E_{\mathrm{UCCSD(T)/cc-pVTZ}}) \quad (1)$$

$$E_{\mathrm{CBSII}} = E_{\mathrm{UCCSD(T)/cc-pVQZ}} + \frac{73}{55}(E_{\mathrm{UCCSD(T)/cc-pVQZ}} - E_{\mathrm{UCCSD(T)/cc-pVTZ}}) + \frac{8}{55}(E_{\mathrm{UCCSD(T)/cc-pVDZ}} - E_{\mathrm{UCCSD(T)/cc-pVTZ}}) \quad (2)$$

where $E_{\mathrm{CBSI}}^{\mathrm{W1}}$ is the energy extrapolated using the W1 theory[32] and the cc-pVQZ and cc-pVTZ basis sets, and E_{CBSII} is the energy extrapolated using the cc-pVDZ, cc-pVTZ, and cc-pVQZ basis sets. Here we extrapolate the HF energy and correlation energy in the same way. This is usually a very accurate approximation. As shown in previous studies,[31−33] the results indicate that this approach can significantly improve the accuracy of the calculated energies, and provide nearly chemically accurate values (relative energies to better than 1 kcal/mol).[31] In the present work, the two extrapolation methods are used to verify the accuracy of our calculations.

Since it is prohibitively formidable to carry out direct ab initio dynamics calculations using the accurate scheme described above, we employ the "scaling all correlation" (SAC) method of Truhlar et al.[35−37] as in our previous work.[34] Here the forces used in classical trajectory propagations are determined by a dual-level ab initio potential energy surface calculation, i.e.,

$$E_{\mathrm{SAC}} = E_{\mathrm{HF}} + \frac{E_{\mathrm{UCCSD}} - E_{\mathrm{HF}}}{F} \quad (3)$$

where E_{HF} and E_{UCCSD} are the Hartree−Fock and coupled-cluster with single and double excitations energies with the cc-pVDZ basis set. The global scaling factor F, which depends on both the method and the basis, is determined to be 0.82 by minimizing the root-mean-square (rms) errors of the SAC energies of the stationary points relative to the CBS II values. The rms errors are obtained as 1.3 kcal/mol. All electronic structure calculations were performed using the Gaussian 03 program.[38]

The dynamics calculations were carried out using the DualOrthGT program.[34] As the procedure has been well described previously, we will not provide any additional details here. Trajectories were propagated with a time step of 0.32 fs for a set of randomly sampled initial conditions,[34,39] where only the collision energy was held at a fixed value. The orientation, rotational energy, and vibrational phases of reactants were selected according to the canonical ensemble at $T = 300$ K. The initial center-of-mass distance between the $^1CH_2$ and C_2H_2 reactants was set as $\rho_0 = \sqrt{R_0^2 + b^2}$ with $R_0 = 14.2$ a_0, where $b = \xi^{1/2} b_{\max}$ is the impact parameter. ξ is an uniformly distributed random number in (0,1), and $b_{\max}$ is the maximum impact parameter. All trajectories were terminated before or at a propagation time of 2 ps. This time is sufficiently long to separate reactive trajectories from nonreactive ones.

Reaction cross sections[40,41] at a collision energy of E_T are calculated as

$$\sigma_r(E_T) = \pi b_{\max}^2 P_r \quad (4)$$

with the reaction probability

$$P_r = N_r/N,\ N_r = N_d + N_c f_r \quad (5)$$

where N_d and N_c are the number of completely reactive and complex-forming trajectories at the time of 2.0 ps of a total of N trajectories. Here the factor f_r is the fraction of intermediates dissociating into the $H + C_3H_3$ products. We have taken $f_r = 1.0$ because, at the conditions of our dynamics simulations, the probability of these long-lived intermediates going back to reactants (after 2.0 ps of trajectory propagation) is negligible based on our variational RRKM calculations using the B3LYP/cc-pVDZ theory. This is consistent with the master equation simulation of Frankcombe and Smith.[15] At collision energies less than 20.0 kcal/mol, there is only one product channel open. Moreover, no completely reactive trajectory at the time $t = 2.0$ ps was obtained here, i.e., $N_d = 0$.

The errors of calculated cross sections can be written as

$$\Delta\sigma_r(E_T) = \pi b_{\max}^2 \left(\frac{N_r(N - N_r)}{N^3}\right)^{1/2} \quad (6)$$

The thermal rate constants are given by

$$k(T) = \left(\frac{8}{\pi\mu(k_B T)^3}\right)^{1/2} \int_0^\infty E_T \sigma_r(E_T) \mathrm{e}^{-E_T/k_B T}\, \mathrm{d}E_T \quad (7)$$

where μ is the reduced mass of the reactants and other symbols have their usual meaning. Finally, the lifetime ($\tau_{c-C_3H_4}$) of the cyclopropene complex is calculated according to its survival probability $P_s(t)$, where the time zero ($t = 0$) is defined by the first c-C_3H_4 molecule formed in each trajectory, as

$$P_s(t) = \mathrm{e}^{-t/\tau_{c-C_3H_4}} \quad (8)$$

Due to the nature of the long lifetime of the allene and propyne complexes, the present dynamics study is not able to calculate their lifetimes with a trajectory propagation of 2.0 ps.

The molecular fragments or shape of the system is identified using graph theory.[42,43] Since graph theory is not widely used in dynamics studies, a concise description will be given here.

TABLE 1: Comparison of Theoretical UCCSD/cc-pVDZ, UCCSD(SAC)/cc-pVDZ, CBSI(W1), and CBSII Energies with Previous Calculations[11−13] and Experimental Enthalpies[44−47] (0 K)[a]

species	UCCSD	SAC	CBSI	CBSII	ZPE	CBSII+ΔZPE	ΔH^0_{0K}44−47	MRCI[11 b]	ICCI[12−13 b]
$^1CH_2$+ C_2H_2	114.35	116.33	118.33	118.62	27.12	110.78	108.06		106.5
H+CH_2CCH	95.0	100.36	99.83	99.77	25.64	90.45	88.96 ± 3.0		
c-C_3H_4	23.12	22.51	23.46	23.37	35.26	23.67	22.34	22.7	25.8
CH_2CCH_2	0.78	0.74	1.36	1.35	34.70	1.09	1.21	0.3	1.7
CH_3CCH	0.0	0.0	0.0	0.0	34.96	0.0	0.0 ± 0.21	0.0	0.0
TS1	68.18	69.95	71.76	71.70	32.17	68.91		66.1	68.9
TS3	63.52	61.57	63.37	63.21	32.60	60.85		60.8	60.8

[a] All energies except for zero-point energies (ZPE) in kcal/mol are relative to the propyne molecule. Energies at the propyne molecule are −116.301138 au for UCCSD/cc-pVDZ, −116.395321 au for UCCSD(SAC)/cc-pVDZ, −116.489596 au for CBSI(W1), and −116.494812 au for CBSII, respectively. [b] Zero-point energy corrections are included.

TABLE 2: Harmonic Frequencies and Rotational Constants of the Stationary Points Calculated with the UCCSD/cc-pVDZ Method

species	frequencies/cm^{-1}	rotational constants/GHz
$^1CH_2$	1418, 2914, 2988	209.40, 333.11, 563.86
C_2H_2	580(2), 755(2), 2030, 3426, 3521	34.331
CH_2CCH	332, 380, 457, 618, 622, 1037, 1064, 1468, 2009, 3185, 3295, 3470	8.9623, 9.2568, 281.71
c-C_3H_4	587, 801, 828, 928, 1017, 1044, 1081, 1103, 1185, 1520, 1715, 3087, 3161, 3283, 3328	13.574, 21.548, 29.359
CH_2CCH_2	353(2), 859(2), 867, 1024(2), 1096, 1437, 1493, 2051, 3167(2), 3259(2)	8.6719, 8.6719, 141.95
CH_3CCH	328(2), 633(2), 948, 1060(2), 1420, 1483(2), 2212, 3073, 3157(2), 3479	8.3407, 8.3407, 156.74
TS1	541*i*, 304, 552, 850, 929, 932, 972, 1077, 1253, 1463, 1676, 2953, 3073, 3186, 3285	9.0323, 10.043, 65.992
TS3	948*i*, 636, 708, 878, 1001, 1039, 1052, 1074, 1242, 1476, 1622, 2395, 3119, 3221, 3343	12.767, 18.390, 32.357

Mathematically a graph[42,43] has only edges and vertexes without any concept of length or angle. Each edge connects two vertexes. A graph is described by a connection table, in which each vertex has been listed by the number of other vertexes connected to it through edges. In this molecular application, a chemical bond is taken as an edge while the atoms correspond to vertexes. For a system of M atoms, a molecular fragment is defined as a subset of atoms that are connected by edges. An edge between atom i and atom j is formed if their bond distance R_{ij} is less than a critical value of α_{ij}. By labeling the atoms in a molecule (in any order), we can construct a symmetric $M \times M$ adjacency matrix $\mathbf{C}$ as

$$\mathbf{C}_{ij} = \begin{cases} 1, \text{ if } R_{ij} < \alpha_{ij} \\ 0, \text{ otherwise} \end{cases} \tag{9}$$

where all edge lengths have a value of unity in the graph representation.

According to graph theory,[42,43] the distance from i to j is determined by an integer p (≥ 1), where the element $\mathbf{C}^p_{ij}$ of the $M \times M$ matrix $\mathbf{C}^p$ ($=\mathbf{C} \times \mathbf{C}^{p-1}$) is nonzero but it is zero in $\mathbf{C}^q_{ij}$ for all positive values of $q < p$. That is, the graph distance between any two atoms i and j is the number of edges on the shortest path connecting i and j. By using this result, we can calculate a new matrix $\mathbf{F}$ as

$$\mathbf{F} = \sum_{k=1}^{M-1} \mathbf{C}^k \tag{10}$$

where the matrix element $\mathbf{F}_{ij}$ is nonzero if and only if atoms i and j are in the same fragment. Therefore the molecular fragments of the system can be identified using the $\mathbf{F}$ matrix. For instance, the $^1CH_2$ + C_2H_2 reactants have two fragments. If one labels the atoms in $^1CH_2$ first for constructing the adjacency $\mathbf{C}$ matrix, the resulting $\mathbf{F}$ ($M = 7$) matrix is block diagonal with two diagonal blocks while the off-diagonal blocks are zero. The leading diagonal block has a size of 3×3 whereas the other block forms a 4×4 matrix. They represent the bond connections in $^1CH_2$ and C_2H_2, respectively. All off-diagonal elements of both diagonal blocks are nonzero.

Similarly, we can use the $\mathbf{C}$ and $\mathbf{C}^2$ matrixes to identify the cyclopropene, allene, and propyne intermediates in terms of the appropriate nonzero matrix elements along the evolution of a trajectory. The identification can be done in three steps. One first finds out whether the collision system is in a single fragment by using the $\mathbf{F}$ matrix in eq 10 at the collision time t. If the geometry corresponds to a chemically bonded molecule, the original $\mathbf{C}$ matrix is then used to determine the connectivity of the three carbon atoms by inspecting the $\mathbf{C}_{ij}$ elements corresponding to the carbon indices. For a given carbon atom i, $\mathbf{C}_{ij}$ will be nonzero only if carbon atom j is connected directly to it, i.e., you can go from atom i to atom j in one jump. For cyclopropene, all three unique off-diagonal elements will be nonzero, while for allene, propyne, or a transient ring-opened intermediate, one of them will be zero. Finally, the connection table for the four hydrogen atoms is constructed using the 4×4 submatrix of the ($\mathbf{C} + \mathbf{C}^2$) matrix, which indicates which hydrogen atoms are attached to the same carbon atom, i.e., which other H atoms can be reached in two jumps from a given H atom. This submatrix will be block-diagonal with the dimension of each block indicating the number of hydrogen atoms attached to a single carbon atom. The possible outcomes are (2,1,1) for cyclopropene or a transient ring-opened intermediate, (2,2) for allene, and (3,1) for propyne. By combining all the information gathered in these steps, one knows the detailed structure of the system. For numerical convenience, we have assigned a unique "tag" to record the configuration of the system at each step of every trajectory. In this work, the fragment tag is set to 3 for propyne, 1 for cyclopropene, −3 for allene, and 0 for all other species as shown below. Of course, the numerical value of the tag is arbitrary, but it allows us to record how much time each trajectory spends in a given configuration of interest. The chemical bond criteria in eq 9 are $\alpha_{HH} = 2.3$ a_0, $\alpha_{CH} = 3.0$ a_0, and $\alpha_{CC} = 3.9$ a_0.

III. Results and Discussion

Calculated energetics for the $^1CH_2 + C_2H_2 \rightarrow H + C_3H_3$ reaction are listed in Table 1, together with a comparison of previous results. Here only the critical stationary points are listed. Their harmonic frequencies and rotational constants are given in Table 2, while the geometries of the TS1 and TS3 transition states are displayed in Figure 1. As one can see, the

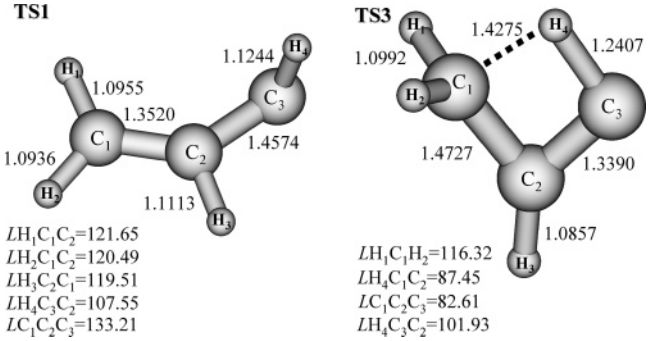

Figure 1. Geometries of the two critical transition states, TS1 and TS3, optimized at the UCCSD/cc-pVDZ level, where lengths are in Å while angles are in deg.

present CBS energies are in good agreement with the available experimental values. Compared to the experimental results,[44−47] the mean absolute deviations of the two CBS calculations are about 1.1 kcal/mol. In addition, the barrier height (68.91 kcal/mol) of the TS1 saddle point is close to that of the ICCI value,[12,13] but is 2.8 kcal/mol higher than that from the MRCI calculation.[11] Most importantly, the UCCSD(SAC)/cc-pVDZ energies are in excellent agreement with the experimental values as well as the CBS results. This agreement validates the use of the UCCSD(SAC)/cc-pVDZ method in the dynamics study.

A schematic energy diagram for the $^1CH_2 + C_2H_2 \rightarrow H + C_3H_3$ reaction is shown in Figure 2. Essentially, this is a barrierless reaction but there are three deep wells involved along the minimum energy path. The relative energies (with zero-point energy corrections included) with respect to the reactants are −87.11 kcal/mol for the cyclopropene, −109.69 kcal/mol for allene, and −110.78 kcal/mol for propyne. Among these three isomers the cyclopropene is the least stable. It can undergo a ring-opening reaction to form either the propyne or allene molecule. The corresponding isomerization barriers are 37.18 and 45.24 kcal/mol, respectively. Both molecules can eliminate a hydrogen atom to form the propargyl radical. The enthalpy (0 K) of the $^1CH_2 + C_2H_2 \rightarrow H + C_3H_3$ reaction is obtained as −20.33 kcal/mol, which is in good agreement with the experimental result[44−47] of −19.1 ± 3.0 kcal/mol.

Figure 3 shows a typical trajectory for the formation of allene.

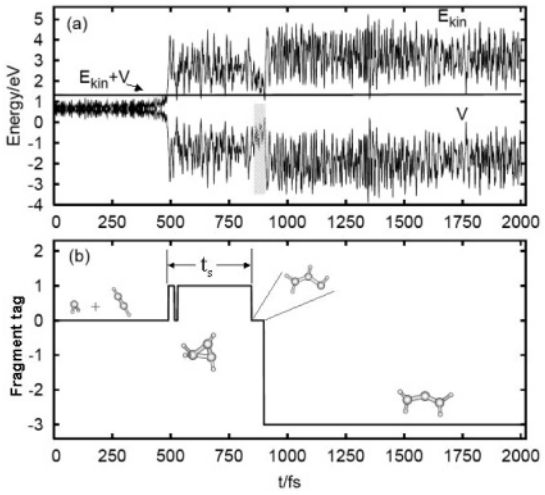

Figure 3. Energy variation and conservation, panel a, and structure evolution, panel b, for a typical $^1CH_2 + C_2H_2 \rightarrow$ c-$C_3H_4 \rightarrow CH_2CCH_2$ (allene) reaction course.

The energy evolution is displayed in Figure 3a, where V is the potential energy with respect to the limit of the reactants and E_{kin} is the kinetic energy including the translational, rotational, and vibrational motion. As one can see, the total energy ($E_{kin} + V$) is well conserved as it follows an essentially horizonal line in the figure. Actually, at this propagation time step, the deviation of the total energy of a trajectory is within 0.5% even though the potential and kinetic energies exhibit severe oscillations.

The trajectory view shown in Figure 3b reveals that allene is formed via a short-lived cyclopropene intermediate. The c-C_3H_4 molecule forms at the time of 480 fs by the addition of $^1CH_2$ to the carbon−carbon triple bond in C_2H_2. As two strong C−C chemical bonds are forming, the potential energy decreases by a large amount as displayed in Figure 3a. Then the potential energy exchanges with the kinetic energy during the course of the reaction. The strong oscillation of the kinetic energy reveals that the c-C_3H_4 is highly energized. Indeed, at the time of 845 fs, one C−C bond breaks to form a less stable intermediate

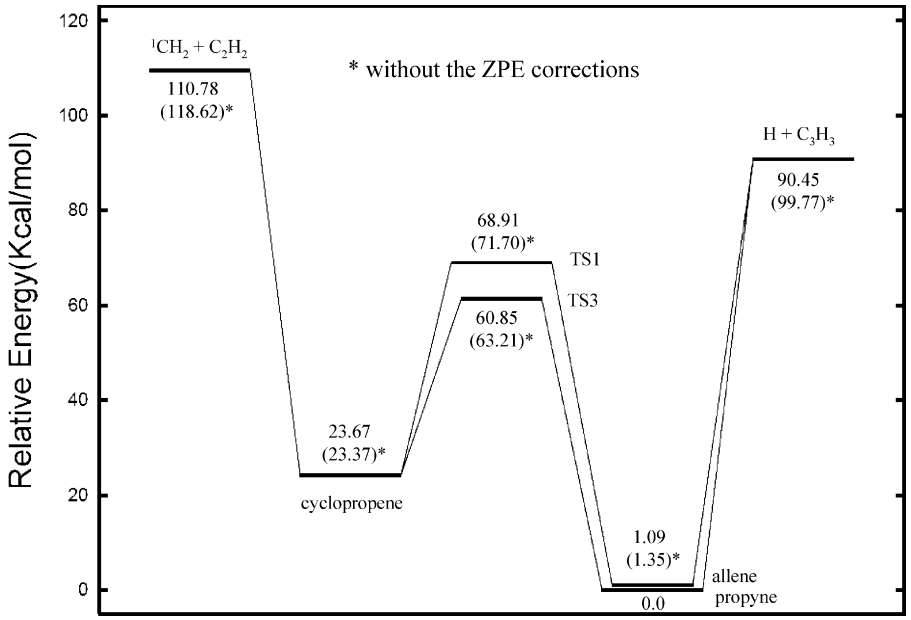

Figure 2. An energy level diagram for the $^1CH_2 + C_2H_2 \rightarrow H + C_3H_3$ reaction calculated with the extrapolated complete basis set method II.

TABLE 3: Calculated Reaction Probabilities (P_r), Reaction Cross Sections (σ_r), and Lifetimes ($\tau_{c-C_3H_4}$) of the Cyclopropene Complex at Five Collision Energies (E_T) in kcal/mol

E_T	b_{max}/a_0	N	N_r	N_c	P_r	σ_r/a_0^2	$\tau_{c-C_3H_4}$/ps	$(N_p, N_a)^a$
0.5	12.5	295	113	110	0.383	188.03 ± 5.32	3.22 ± 0.26	(10, 14)
1.5	9.5	371	118	116	0.318	90.18 ± 2.18	2.93 ± 0.83	(16, 17)
5.0	7.0	290	101	98	0.343	53.61 ± 1.50	3.38 ± 0.25	(22, 13)
10.0	6.5	264	85	82	0.322	42.74 ± 1.23	3.38 ± 0.50	(14, 14)
20.0	5.5	288	100	93	0.347	33.00 ± 0.93	3.00 ± 0.24	(26, 25)

[a] N_p and N_a are the numbers of the trajectories forming cyclopropene complexes that decay into propyne and allene, respectively, within an overall reaction time of 2.0 ps.

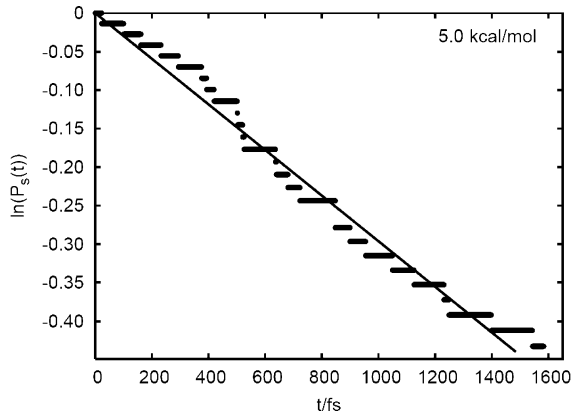

Figure 4. A logarithm plot of the survival probability ($P_s(t)$) of the cyclopropene complex as a function of time at a collision energy of 5.0 kcal/mol.

(CH_2CHCH). As shown in Figure 3a by the shaded rectangle, its mean potential energy is higher than that of the cyclopropene complex. The CH_2CHCH intermediate survives only about 55 fs. Through a 1,2 H-shift reaction of the hydrogen atom connected to the middle carbon, a more stable allene intermediate finally appears. The energized allene has a long liftetime for dissociation to H + C_3H_3. We can calculate the survival time (indicated by "t_s" in Figure 3b) of the cyclopropene complex in this trajectory. The survival time is measured by the interval between the initial formation and final decay of c-C_3H_4.

From a batch of such trajectories, we can obtain the statistical survival probability $P_s(t) = N_s(t)/N_c$ at time t. Here N_c is the total number of trajectories forming the c-C_3H_4 complex and $N_s(t)$ is the number of surviving trajectories at the time t. According to eq 8, the plot of the logarithm of $P_s(t)$ against t is a straight line. Such a plot is given in Figure 4 for a collision energy of 5.0 kcal/mol. Conceptually, it is constructed by making an ordered list of the intermediate lifetimes sorted from shortest to longest. At time zero, all N_c trajectories are surviving, so the survival probability is unity. The survival probability remains unity until the time of the first entry in the list (corresponding to the shortest lifetime in the ensemble), when it drops by $1/N_c$. It remains constant again until the time of the second entry in the list, when it drops by another $1/N_c$. The resulting histogram of $\ln(P_s(t))$ vs t approximates a straight line with slope $-1/\tau_{c-C_3H_4}$ and intercept 0. The results obtained for five collision energies are listed in Table 3. No apparent energy dependence is observed (consistent with the collision energy being a relatively small fraction of the energy available to the cyclopropene complex), and the mean lifetime is predicted to be 3.18 ± 0.42 fs. This predicted lifetime is somewhat shorter than the RRKM values[13] of 3.7−4.1 ps. In addition, by keeping account of the ultimate fate of the ensemble of c-C_3H_4 trajectories, we can estimate the branching ratio of propyne to allene as nearly unity, as given in Table 3. At lower collision energies, the allene product is slightly preferred. On the other hand, the propyne is favored at higher collision energy.

Table 3 also summarizes other important dynamics results. First, the maximum impact parameter decreases with increasing collision energy. This implies that the long-range interaction force plays an important role in this barrierless reaction. Second, we note that there are two mechanisms for the formation of propyne. One occurs along the pathway in which the propyne molecule is produced through a ring-opening of the cyclopropene complex similar to the formation of allene. The other is the direct insertion of the $^1CH_2$ reactant into a H−C bond of C_2H_2. However, the probability of the latter mechanism, as indicated by $(N_r - N_c)$ in Table 3, is rather small but obviously finite. Furthermore, it seems that the direct insertion reaction tends to be more important at the higher collision energies.

To better understand these two mechanisms, we have plotted two representative trajectories, one illustrating each mechanism, in Figure 5. Here the orientation and the center-of-mass of the collision system are fixed throughout each trajectory, but the time intervals between frames are not the same in order to show the critical configurations. As shown in Figure 5a, when the $^1CH_2$ molecule approaches the C_2H_2 molecule, one hydrogen atom in acetylene starts to transfer to the methylene molecule at $t = 604$ fs. This abstraction process occurs within a few femtoseconds. The resulting methyl radical then quickly inverts its umbrella mode, and adds to the terminal carbon of the resulting CCH radical to form the propyne molecule. This step occurs over tens of femtoseconds. Here the umbrella inversion is necessary for the development of an sp^3 hybrid orbital on the methyl radical to overlap with the sp hybrid orbital on the CCH radical to form a C−C single bond. The original C−C triple bond remains intact throughout the reaction. Finally, the newly formed propyne vibrates and rotates in space, and eventually would dissociate into products if we could propagate the trajectory for a sufficiently long time. For this particular trajectory, the rotational period can be estimated as 1.6 ps. Finally, it is difficult to distinguish whether this is an insertion or an abstraction/addition reaction. While it has been described here as the latter, the reaction appears to be concerted, with the lighter hydrogen atom forming a new bond first because it is moving faster. In this respect, this mechanism is similar to that of the $O(^1D)$ insertion into a C−H bond of methane.[34]

Figure 5b displays the normal addition/ring-opening mechanism. While the methylene molecule approaches the acetylene molecule, a cyclopropene intermediate is formed first. Owing to a large decrease in potential energy, the complex undergoes large-amplitude vibrational motion while rotating. Even the C_3 ring can be temporarily broken (breaking a C−C single bond) as shown at $t = 539$ and 1276 fs. If at the instant of this ring opening the terminal H on what was initially acetylene moves toward the other end of the C−C−C chain, a 1,3 H-shift reaction will rapidly occur, as shown in the figure at $t = 1284-1296$ fs. Then the CH_3CHC species undergoes a 1,2 H-shift at $t = 1329$ fs to yield the propyne molecule. The system continues to rotate,

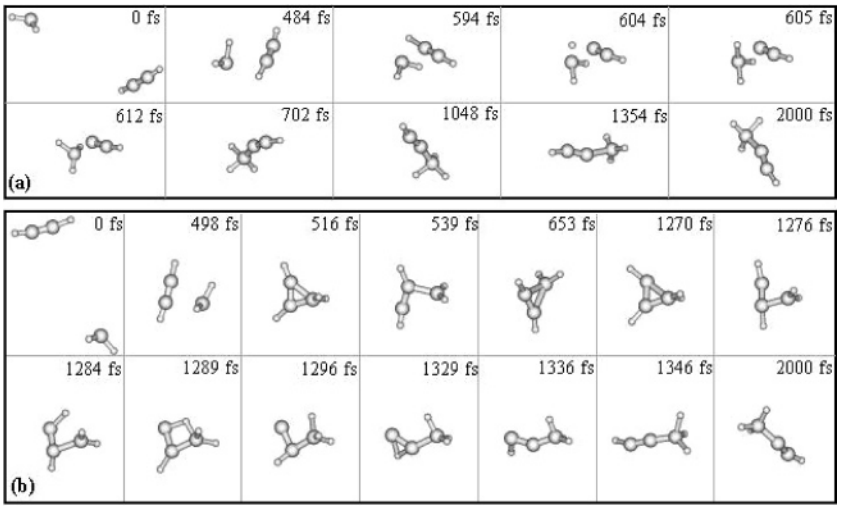

Figure 5. Two typical trajectories for the formation of propyne: (a) a direct abstraction/addition mechanism and (b) a normal addition/ring-opening mechanism.

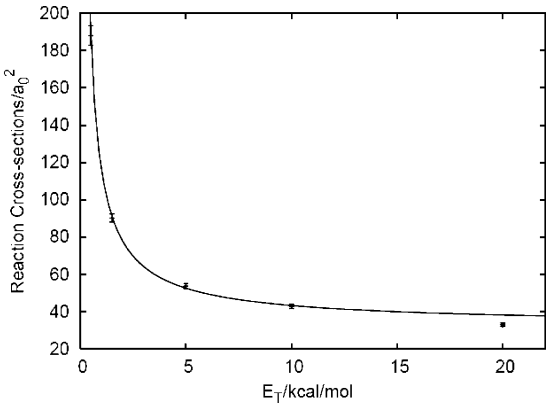

Figure 6. Calculated cross sections (filled squares with error bars) and their fitting curve (solid line) for the $^1CH_2 + C_2H_2 \rightarrow H + C_3H_3$ reaction.

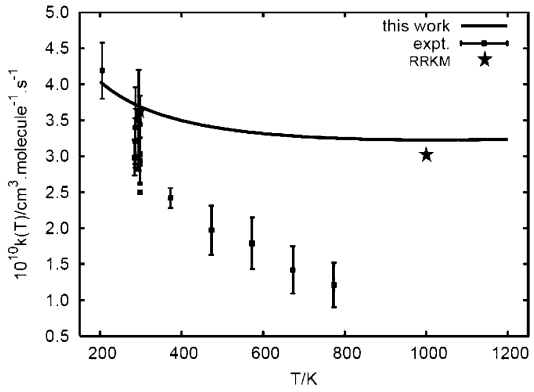

Figure 7. Comparison of these rate constants (solid line) with previous experimental results[16−21] (filled squares with/without error bars) and the RRKM calculations[13] (stars).

but with a longer period than the c-C_3H_4 complex because propyne has larger moments of inertia than cyclopropene. In this mechanism, the original C−C triple bond in acetylene first becomes the double bond in cyclopropene, and then the triple bond in propyne.

Calculated reaction cross sections are shown in Figure 6 and are listed in Table 3. As described in Section II, here only capture cross sections is computed although all possible reaction channels are included in the dynamics calculations. The cross sections sharply increase as the collision energy approaches zero. These results are well fit by the function of $\sigma_r(E_T) = \sigma_0 + \sigma_1/E_T^{\alpha}$ with $\sigma_0 = 32.1889$, $\sigma_1 = 84.1314$, and $\alpha = 0.881885$ in the units of a_0 and kcal/mol. Here we have given a large weight to the low-energy points. The fitted curve is also displayed in the figure. The agreement is very good. Using this function, we can compute the thermal rate constants analytically as

$$k(T) = \left(\frac{8k_BT}{\pi\mu}\right)^{1/2}\left\{\sigma_0 + \frac{\sigma_1\Gamma(2-\alpha)}{(k_BT)^{\alpha}}\right\} \qquad (11)$$

where $\Gamma(x)$ is the Gamma function. The rate constants obtained are listed in Table 4.

Figure 7 shows a comparison of these rate constants with previous results. At room temperature, we obtain a rate constant of $(3.70 \pm 0.08) \times 10^{-10}$ cm^3 molecule^{-1} s^{-1}, which is in good agreement with the experimental values[16−21] of $(2.5-3.7) \times 10^{-10}$ cm^3 molecule^{-1} s^{-1} as well as the RRKM value[13] of 3.6 $\times 10^{-10}$ cm^3 molecule^{-1} s^{-1}. Studies of the temperature dependence of the reaction rate constants are scarce. There is only one kinetic measurement for the overall reaction rate by Blitz and co-workers.[16] Compared to their observations, our calculations are larger by a factor of 3 at higher temperatures although the agreement is very good at temperatures below room temperature. The differences exceed our statistical deviations as given in Table 4. It is not clear whether the discrepancy arises from the theoretical treatment or the kinetic measurements, or even both. The theoretical errors may arise from the accuracy of the ab initio method employed. Since this is a barrierless reaction, the quasiclassical trajectory simulation usually works well.

TABLE 4: Calculated Thermal Rate Constants $k(T)$ in cm^3 molecule^{-1} s^{-1} for the $^1CH_2 + C_2H_2 \rightarrow H + C_3H_3$ Reaction

T/K	$10^{10}k(T)$	T/K	$10^{10}k(T)$
200	4.04 ± 0.14	350	3.58 ± 0.06
225	3.92 ± 0.12	400	3.50 ± 0.05
250	3.83 ± 0.10	500	3.38 ± 0.04
275	3.75 ± 0.09	600	3.31 ± 0.03
298	3.70 ± 0.08	800	3.24 ± 0.03
300	3.68 ± 0.08	1000	3.23 ± 0.03
		1200	3.23 ± 0.04

In addition, Guadagnini et al.[13] have predicted a rate constant of 3.0×10^{-10} cm^3 molecule^{-1} s^{-1} at $T = 1000$ K using RRKM theory, which is close to our calculated value of $(3.23 \pm 0.03) \times 10^{-10}$ cm^3 molecule^{-1} s^{-1}. Quite recently, Davis and co-

workers[22] have studied the $^1CH_2 + C_2H_2 \rightarrow H + C_3H_3$ reaction using the method of crossed molecular beams at a mean collision energy of 3.0 kcal/mol. The propargyl radical products were directly measured using a single photon ionization technique. By using the fitting function, $\sigma_r(E_T)$, we can calculate the reaction cross-sections as 64.12 a_0^2 at $E_T = 3.0$ kcal/mol. Then the corresponding rate constant is $k_E = \upsilon_r\sigma_r(E) = 2.98 \times 10^{-10}$ cm^3 $molecule^{-1}$ s^{-1}, where υ_r is the collision speed. In terms of the statistical relationship $\upsilon_r = (8k_BT/\pi\mu)^{1/2}$, we can estimate the collision temperature as $T = 1086$ K.

IV. Conclusions

We have refined the energetics of the critical stationary points for the $^1CH_2 + C_2H_2 \rightarrow H + C_3H_3$ reaction using an extrapolated complete basis set theory. The reaction dynamics have also been carried out employing an accurate dual-level "scaling all correlation" ab initio method, i.e., UCCSD(SAC)/cc-pVDZ. Graph theory has been applied for identifying the fragments or the shape of the collision system during the course of reaction. The results show that the reaction cross sections increase dramatically as the collision energy approaches zero. As a result, the reaction rate constants have a negative temperature dependence, which is consistent with the kinetic experiments of Blitz et al.[16] Generally, the calculated thermal rate constants are in good agreement with previous measurements, but display an apparent discrepancy with those of Blitz et al.[16] at high temperatures. The lifetime of the cyclopropene intermediate is predicted to be 3.18 ± 0.42 fs. The cyclopropene complex has nearly equal probability to isomerize either to allene or propyne. Higher collision energies may slightly drive the cyclopropene molecule to form propyne, lower ones to form allene. Furthermore, we have provided concrete evidence that the propyne radical can be formed through an insertion (or abstraction/addition) reaction of $^1CH_2$ with a C−H bond in C_2H_2. This mechanism has some different aspects from the well-known addition mechanism as shown in Figure 5b. However, compared to the normal addition pathway, such a mechanism is of much less importance. Finally, the quenching reaction of $^1CH_2$ to $^3CH_2$ by the partner C_2H_2 was not explicitly studied here, but may be "accounted for" in the calculated capture cross sections. This reaction may play an important role in combustion environments.

Acknowledgment. We thank Dr. Mark A. Blitz for bringing this reaction to our attention. This work was performed at Brookhaven National Laboratory under Contract No. DE-AC02-98CH10886 with the U.S. Department of Energy and supported by its Division of Chemical Sciences, Office of Basic Energy Sciences.

References and Notes

(1) Westmoreland, P. R.; Dean, A. M.; Howard, J. B.; Longwell, J. P. *J. Phys. Chem.* **1989**, *93*, 8171.

(2) Miller, J.A.; Melius, C.F. *Combust. Flame* **1992**, *91*, 21.

(3) Leung, K. M.; Lindstedt, R. P. *Combust. Flame* **1995**, *102*, 129.

(4) Fahr, A.; Nayak, A. *Int. J. Chem. Kinetics* **2000**, *32*, 118.

(5) Alkemade, U.; Homann, K. H. *Z. Phys. Chem.* **1989**, *161*, 19.

(6) Miller, J. A.; Klippenstein, S. J. *J. Phys. Chem. A* **2001**, *105*, 7254.

(7) DeSain, J. D.; Taatjes, C. A. *J. Phys. Chem. A* **2003**, *107*, 4843.

(8) Shafir, E. V.; Slagle, I. R.; Knyazev, V. D. *J. Phys. Chem. A* **2003**, *107*, 8893.

(9) Honjou. N.; Pacansky, J.; Yoshimine, M. *J. Am. Chem. Soc*. **1984**, *106*, 5361.

(10) Honjou. N.; Pacansky, J.; Yoshimine, M. *J. Am. Chem. Soc*. **1985**, *107*, 5332.

(11) Yoshimine, M.; Pacansky, J.; Honjou. N. *J. Am. Chem. Soc*. **1989**, *111*, 2785, 4198.

(12) Walch, S. P. *J. Chem. Phys.* **1995**, *103*, 7064.

(13) Guadagnini, R.; Schatz, G. C.; Walch, S. P. *J. Phys. Chem. A* **1998**, *102*, 5857.

(14) Kiefer, J. H.; Mudipalli, P. S.; Sidhu, S. S.; Kern, R. D.; Jursic, B. S.; Xie, K.; Chen, H. *J. Phys. Chem. A* **1997**, *101*, 4057.

(15) Frankcombe, T. J.; Smith, S. C. *J. Chem. Phys.* **2003**, *119*, 12729.

(16) Blitz, M. A.; Beasley, M. S.; Pilling, M. J.; Robertson, S. H. *Phys. Chem. Chem. Phys.* **2000**, *2*, 805.

(17) Canosa-Mas, C. E.; Frey, H. M.; Walsh, R. *J. Chem. Soc., Faraday Trans. 2* **1985**, *81*, 283.

(18) Bohland, T.; Temps, F.; Wagner, H. G. *Ber. Bunsen-Ges. Phys. Chem.* **1985**, *89*, 1013.

(19) Hack, W.; Koch, M.; Wagner, H. G.; Wilms, A. *Ber. Bunsen-Ges. Phys. Chem.* **1988**, *92*, 674.

(20) Hayes, F.; Gutsche, G. J.; Lawrance, D.; Staker, W. S.; King, K. D. *Combus. Flame* **1995**, *100*, 653.

(21) Adamson, J. D.; Morter, C. L.; DeSain, J. D.; Glass, G. P.; Curl, R. F. *J. Phys. Chem.* **1996**, *100*, 2125.

(22) Davis, H. F.; Shu, J.; Peterka, D. S.; Ahmed, M. *J. Chem. Phys.* **2004**, *121*, 6254.

(23) Cizek, J. *Adv. Chem. Phys*. **1969**, *14*, 35.

(24) Purvis, G. D.; Bartlett, R. J. *J. Chem. Phys.* **1982**, *76*, 1910.

(25) Scuseria, G. E.; Janssen, C. L.; Schaefer, H. F., III *J. Chem. Phys.* **1988**, *89*, 7382.

(26) Dunning, T. H., Jr. *J. Chem. Phys.* **1989**, *90*, 1007.

(27) Pople, J. A.; Head-Gordon, M.; Raghavachari, K. *J. Chem. Phys.* **1987**, *87*, 5968.

(28) Woon, D. E.; Dunning, T. H., Jr. *J. Chem. Phys.* **1993**, *98*, 1358.

(29) Halkier, A.; Helgaker, T.; Jorgensen, P.; Klopper, W.; Koch, H.; Olsen, J.; Wilson, A. K. *Chem. Phys. Lett*. **1998**, *286*, 243.

(30) Helgaker, T.; Klopper, W.; Koch, H.; Noga, J. *J. Chem. Phys*. **1997**, *106*, 9639.

(31) Klopper, W.; Bak, K. L.; Jorgensen, P.; Olsen, J.; Helgaker, T. *J. Phys. B* **1999**, *32*, R103.

(32) Martin, J. M. L.; de Oliveira, G., *J. Chem. Phys.* **1999**, *111*, 1843.

(33) Yu, H.-G.; Muckerman, J. T. *J. Phys. Chem. A* **2004**, 108, 10844.

(34) Yu, H.-G.; Muckerman, J. T. *J. Phys. Chem A.* **2004**, 108, 8615.

(35) Gordon, M. S.; Truhlar, D. G. *J. Am. Chem. Soc.* **1986**, *108*, 5412.

(36) Gordon, M. S.; Truhlar, D. G. *Int. J. Quantum Chem*. **1987**, *31*, 81.

(37) Gordon, M. S.; Nguyen, K. A.; Truhlar, D. G. *J. Phys. Chem*. **1989**, *93*, 7356.

(38) Frisch, M. J.; Trucks, G. W.; Schlegel, H. B.; Scuseria, G. E.; Robb, M. A.; Cheeseman, J. R.; Montgomery, J. A., Jr.; Vreven, T.; Kudin, K. N.; Burant, J. C.; Millam, J. M.; Iyengar, S. S.; Tomasi, J.; Barone, V.; Mennucci, B.; Cossi, M.; Scalmani, G.; Rega, N.; Petersson, G. A.; Nakatsuji, H.; Hada, M.; Ehara, M.; Toyota, K.; Fukuda, R.; Hasegawa, J.; Ishida, M.; Nakajima, T.; Honda, Y.; Kitao, O.; Nakai, H.; Klene, M.; Li, X.; Knox, J. E.; Hratchian, H. P.; Cross, J. B.; Adamo, C.; Jaramillo, J.; Gomperts, R.; Stratmann, R. E.; Yazyev, O.; Austin, A. J.; Cammi, R.; Pomelli, C.; Ochterski, J. W.; Ayala, P. Y.; Morokuma, K.; Voth, G. A.; Salvador, P.; Dannenberg, J. J.; Zakrzewski, V. G.; Dapprich, S.; Daniels, A. D.; Strain, M. C.; Farkas, O.; Malick, D. K.; Rabuck, A. D.; Raghavachari, K.; Foresman, J. B.; Ortiz, J. V.; Cui, Q.; Baboul, A. G.; Clifford, S.; Cioslowski, J.; Stefanov, B. B.; Liu, G.; Liashenko, A.; Piskorz, P.; Komaromi, I.; Martin, R. L.; Fox, D. J.; Keith, T.; Al-Laham, M. A.; Peng, C. Y.; Nanayakkara, A.; Challacombe, M.; Gill, P. M. W.; Johnson, B.; Chen, W.; Wong, M. W.; Gonzalez, C.; Pople, J. A. *Gaussian 03*, revision B.01; Gaussian, Inc.: Pittsburgh, PA, 2003.

(39) Hase, W. L. In *Encyclopedia of Computational Chemistry*; Schleyer, P. v. R., Ed.; John Wiley & Sons: New York, 1998.

(40) Faist, M. B.; Muckerman, J. T.; Schubert, F. E. *J. Chem. Phys.* **1978**, *69*, 4087.

(41) Muckerman, J. T.; Faist, M. B. *J. Phys. Chem.* **1979**, *83*, 79.

(42) Wilson, R. J. *Introduction to Graph Theory*; Longman: London, UK, 1972.

(43) West, D. B. *Introduction to Graph Theory*; Prentice Hall: Englewood Cliffs, NJ, 1996.

(44) Pedley, J. B.; Naylor, R. D.; Kirby, S. P. *Thermochemical Data of Organic Compounds*, 2nd ed.; Chapman and Hall: London, UK, 1986.

(45) Robinson, M. S.; Polak, M. L.; Bierbaum, V. M.; Depuy, C. H.; Lineberger, W. C. *J. Am. Chem. Soc*. **1995**, *117*, 6766.

(46) *JANAF Themochemical Tables*; Natl. Stand. Ref. Data Ser.; U.S. National Bureau of Standards: Washington, DC, 1985; No. 14.

(47) NIST Chemistry WebBook, NIST Standard Reference Database: http://webbook.nist.gov.